

Buckling of Transversely Framed Panels

FRP laminates generally have ultimate tensile and compressive strengths that are comparable with mild steel but stiffness is usually only 5% to 10%. A dominant design consideration then becomes elastic instability under compressive loading. Analysis of the buckling behavior of FRP grillages common in ship structures is complicated by the anisotropic nature of the materials and the stiffener configurations typically utilized. Smith [3-17] has developed a series of data curves to make approximate estimates of the destabilizing stress, σ_x , required to produce catastrophic failure in transversely framed structures (see Figure 3-70).

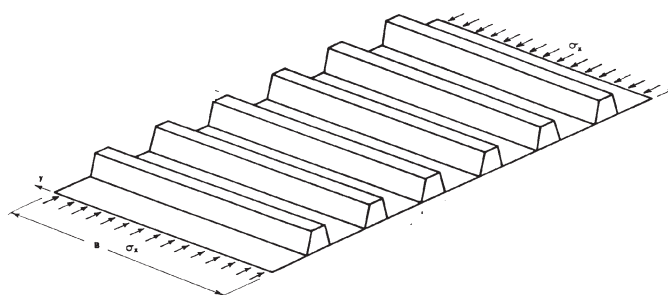


Figure 3-70 Transversely Stiffened Panel [Smith, *Buckling Problems in the Design of Fiberglass Reinforced Plastic Ships*]

The lowest buckling stresses of a transversely framed structure usually correspond to one of the interframe modes illustrated in Figure 3-71.

The first type of buckling (a) involves maximum flexural rotation of the shell/stiffener interface and minimal displacement of the actual stiffener.

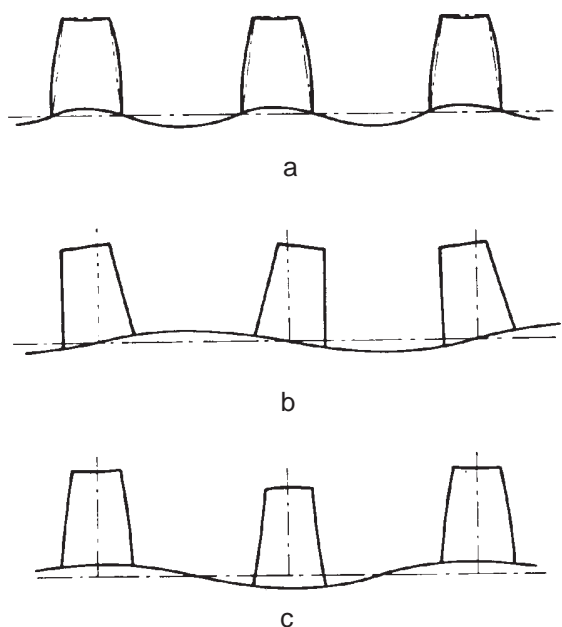


Figure 3-71 Interframe Buckling Modes [Smith, *Buckling Problems in the Design of Fiberglass Plastic Ships*]

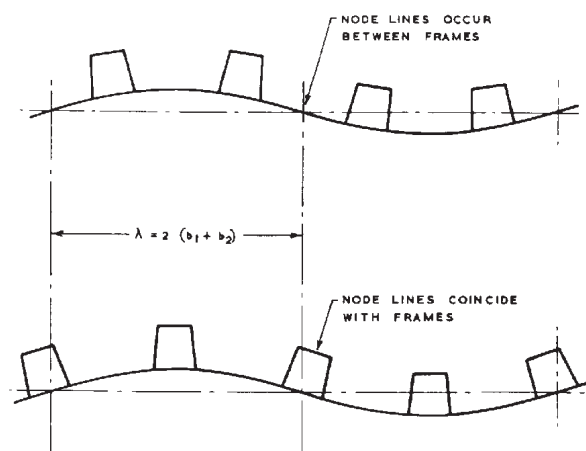


Figure 3-72 Extraframe Buckling Modes [Smith, *Buckling Problems in the Design of Fiberglass Plastic Ships*]

This action is dependent upon the restraining stiffness of the stiffener and is independent of the transverse span.

The buckling phenomena shown in (b) is the result of extreme stiffener rotation, and as such, is a function of transverse span which influences stiffener torsional stiffness.

The third type of interframe buckling depicted (c) is unique to FRP structures, but can often proceed the other failure modes. In this scenario, flexural deformation of the stiffeners produces bending of the shell plating at a half-wavelength coincident with the stiffener spacing. Large, hollow top-hat stiffeners can cause this effect. The restraining influence of the stiffener as well as the transverse span length are factors that control the onset of this type of buckling. All buckling modes are additionally influenced by the stiffener spacing and dimensions and the flexural rigidity of the shell.

Buckling of the structure may also occur at half-wavelengths greater than the spacing of the stiffeners. The next mode encountered is depicted in Figure 3-72 with nodes at or between stiffeners. Formulas for simply supported orthotropic plates show good agreement with more rigorous folded-plate analysis in predicting critical loads for this type of failure. [3-17] The approximate formula is:

$$N_{xcr} = \frac{\pi^2 D_y}{B^2} \left[\frac{D_1 B^2}{D_y \lambda^2} + \frac{2D_{xy}}{D_y} + \frac{\lambda^2}{B^2} \right] \quad (3-85)$$

where:

N_{xcr} = critical load per unit width

D_y = flexural rigidity per unit width

D_1 = flexural rigidity of the shell in the x-direction

D_{xy} = stiffened panel rigidity = $\frac{1}{2}(C_x + C_y)$ with C_y = torsional rigidity per unit width and C_x = twisting rigidity of the shell (first term is dominant)

λ = buckling wavelength

Longitudinally framed vessels are also subject to buckling failure, albeit at generally higher critical loads. If the panel in question spans a longitudinal distance L , a suitable formula for estimating critical buckling stress, σ_{ycr} , based on the assumption of simply supported end conditions is:

$$\sigma_{ycr} = \frac{\frac{\pi^2 EI}{AL^2}}{1 + \frac{\pi^2 EI}{L^2 GA_s}} \quad (3-86)$$

where:

EI = flexural rigidity of a longitudinal with assumed effective shell width

A = total cross-sectional area of the longitudinal including effective shell

GA_s = shear rigidity with A_s = area of the stiffener webs

Buckling failure can occur at reduced primary critical stress levels if the structure is subjected to orthogonal compressive stresses or high shear stresses. Areas where biaxial compression may occur include side shell where lateral hydrodynamic load can be significant or in way of frames that can cause secondary transverse stress. Areas of high shear stress include side shell near the neutral axis, bulkheads and the webs of stiffeners.

Large hatch openings are notorious for creating stress concentrations at their corners, where stress levels can be 3-4 times greater than the edge midspan. Large cut-outs reduce the compressive stability of the grillage structure and must therefore be carefully analyzed. Smith [3-17] has proposed a method for analyzing this portion of an FRP vessel whereby a plane-stress analysis is followed by a grillage buckling calculation to determine the distribution of destabilizing forces (see Figure 3-73). Figure 3-74 shows the first two global failure modes and associated average stress at the structure's mid-length.

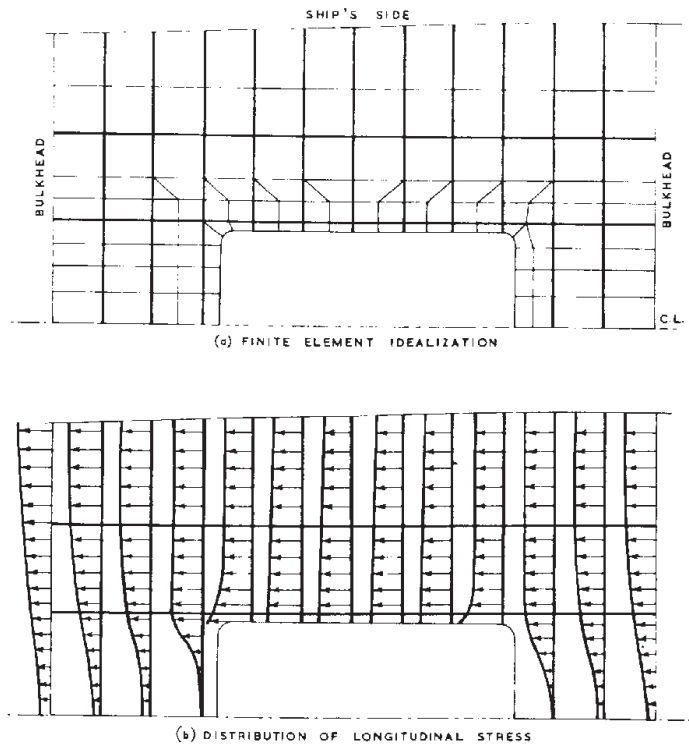


Figure 3-73 Plane Stress Analysis of Hatch Opening [Smith, Buckling Problems in the Design of Fiberglass Plastic Ships]

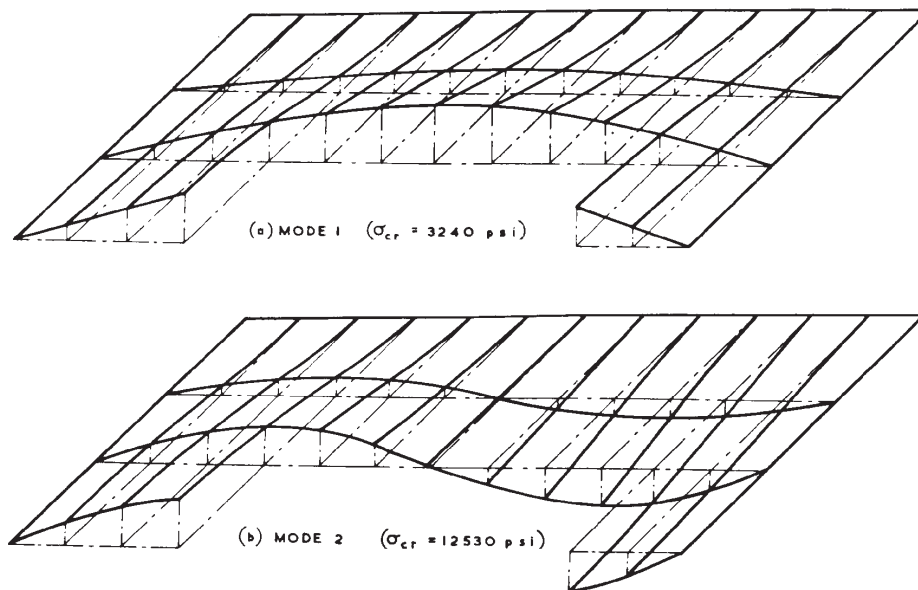


Figure 3-74 Deck Grillage Buckling Modes Near Hatch Opening [Smith, Buckling Problems in the Design of Fiberglass Plastic Ships]

Joins and Details

In reviewing the past four decades of FRP boat construction, very few failures can be attributed to the overall collapse of the structure due to primary hull girder loading. This is in part due to the fact that the overall size of FRP ships has been limited, but also because safety factors have been very conservative. In contrast to this, failures resulting from what is termed “local phenomena” have been observed in the early years of FRP development. As high-strength materials are introduced to improve vessel performance, the safety cushion associated with “bulky” laminates diminishes. As a consequence, the FRP designer must pay careful attention to the structural performance of details.

Details in FRP construction can be any area of the vessel where stress concentrations may be present. These typically include areas of discontinuity and applied load points. As an example, failures in hull panels generally occur along their edge, rather than the center. [3-18] FRP construction is particularly susceptible to local failure because of the difficulty in achieving laminate quality equal to a flat panel. Additionally, stress concentration areas typically have distinct load paths which must coincide with the directional strengths of the FRP reinforcing material. With the benefit of hindsight knowledge and a variety of reinforcing materials available today, structural detail design can rely less on “brute force” techniques.

Secondary Bonding

FRP structures will always demonstrate superior structural properties if the part is fabricated in one continuous cycle without total curing of intermediate plies. This is because interlaminar properties are enhanced when a chemical as well as mechanical bond is present. Sometimes the part size, thickness or manufacturing sequence preclude a continuous lay-up, thus requiring the application of wet plies over a previously cured laminate, known as secondary bonding. Much of the test data available on secondary bonding performance dates back to the early 1970's when research was active in support of FRP minesweeper programs. Frame and bulkhead connections were targeted as weak points when large hulls were subjected to extreme shock from detonated charges. Reports on secondary bond strength by Owens-Corning Fiberglas [3-19] and Della Rocca & Scott [3-20] are summarized below:

- Failures were generally cohesive in nature and not at the bond interface line. A clean laminate surface at the time of bonding is essential and can best be achieved by use of a peeling ply. A peeling ply consists of a dry piece of reinforcement (usually cloth) that is laid down without being wetted out. After cure, this strip is peeled away, leaving a rough bonding surface with raised glass fibers;
- Filleted joints proved to be superior to right-angle joints in fatigue tests. It was postulated that the bond angle material was stressed in more of a pure flexural mode for the radiused geometry;
- Bond strengths between plywood and FRP laminates is less than that of FRP itself. Secondary mechanical fasteners might be considered;
- In a direct comparison between plywood frames and hat-sectioned stiffeners, the stiffeners appear to be superior based on static tests; and
- Chopped strand mat offers a better secondary bond surface than woven roving.

Table 3-6 Secondary Bond Technique Desirability [Della Rocca and Scott, *Materials Test Program for Application of Fiberglass Plastics to U.S. Navy Minesweepers*]

Preferable Bonding Techniques	Acceptable Bonding Techniques	Undesirable Procedures
Bond resin: either general purpose or fire retardant, resilient Surface treatment: roughened with a pneumatic saw tooth hammer, peel ply, or continuous cure of rib to panel; one ply of mat in way of bond Stiffener faying flange thickness: minimum consistent with rib strength requirement Bolts or mechanical fasteners are recommended in areas of high stress	Bond resin: general purpose or fire retardant, rigid air inhibited Surface treatment: rough sanding	No surface treatment Excessive stiffener faying flange thickness

Hull to Deck Joints

Since the majority of FRP vessels are built with the deck and hull coming from different molds, the builder must usually decide on a suitable technique for joining the two. Since this connection is at the extreme fiber location for both vertical and transverse hull girder loading, alternating tensile and compressive stresses are expected to be at a maximum. The integrity of this connection is also responsible for much of the torsional rigidity exhibited by the hull. Secondary deck and side shell loading shown in Figure 3-75 is often the design limiting condition. Other design considerations include: maintaining watertight integrity under stress, resisting local impact from docking,

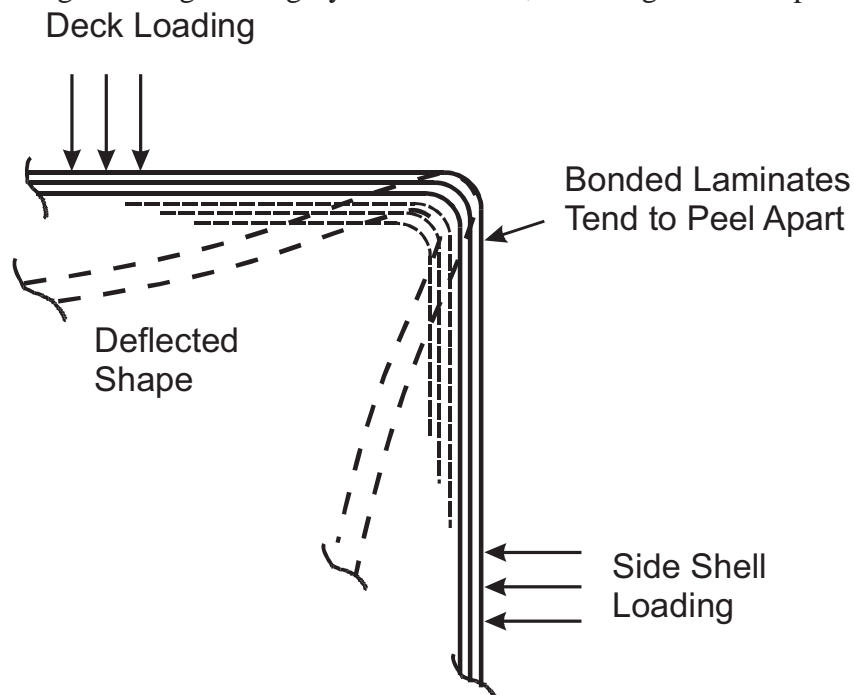
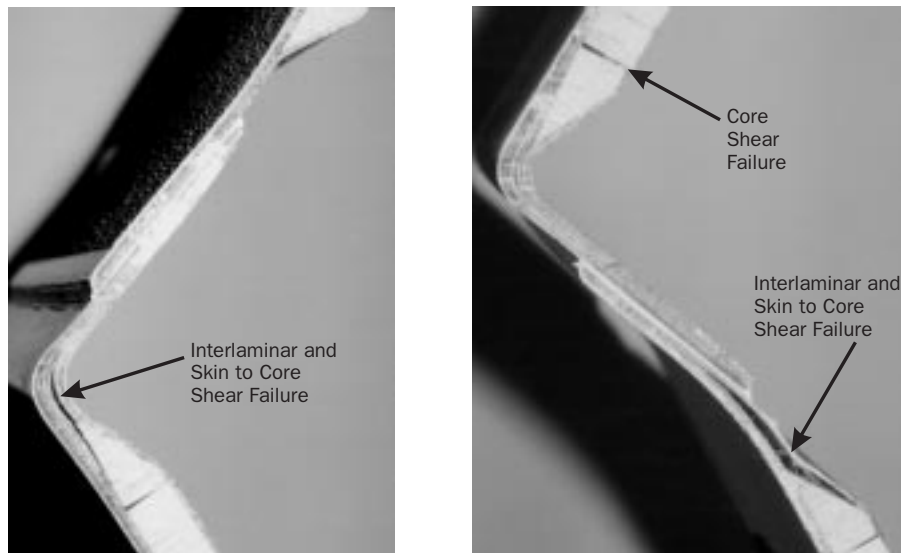


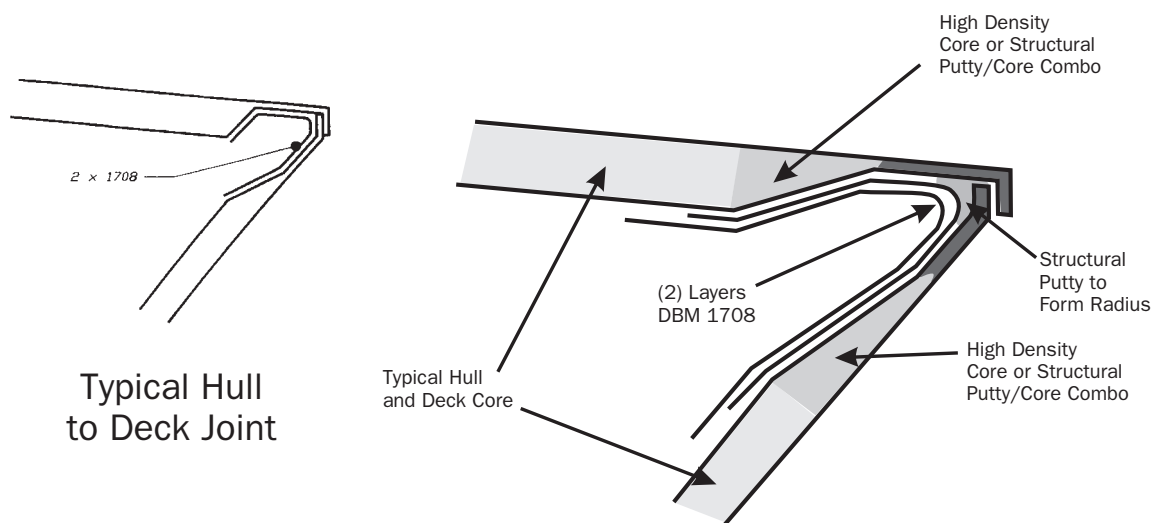
Figure 3-75 Deck Edge Connection - Normal Deck and Shell Loading Produces Tension at the Joint [Gibbs and Cox, *Marine Design Manual for FRP*]

personnel footing assistance, and appearance (fairing of shear). Figure 3-76 shows typical failure modes for traditional sandwich construction with tapered cores. A suggested method for improving hull-to-deck joints is also presented. Transfer of shear loads between inner and outer skins is critical. Note that the lap joint, which used a methacrylate adhesive with a shear strength of 725 psi (50 kg/cm²) did not fail. This compares with polyester resin, which will typically provide 350 psi (24 kg/cm²) and epoxy resin, which provides 500 psi (34.5 kg/cm²) shear strength. [3-21]

Improved Hull to Deck Joint



Typical Failures in Tapered Sandwich Joint Configuration



Suggested Improved Hull to Deck Joint

Figure 3-76 Improved Hull to Deck Joint for Sandwich Core Production Vessels

Bulkhead Attachment

The scantlings for structural bulkheads are usually determined from regulatory body requirements or first principals covering flooding loads and in-plane deck compression loads. Design principals developed for hull panels are also relevant for determining required bulkhead strength. Of interest in this section is the connection of bulkheads or other panel stiffeners that are normal to the hull surface. In addition to the joint strength, the strength of the bulkhead and the hull in the immediate area of the joint must be considered. Other design considerations include:

- Some method to avoid creation of a “hard” spot should be used;
- Stiffness of joint should be consistent with local hull panel;
- Avoid laminating of sharp, 90° corners;
- Geometry should be compatible with fabrication capabilities; and
- Cutouts should not leave bulkhead core material exposed.

An acceptable configuration for use with solid FRP hulls is shown in Figure 3-77. As a general rule, tape-in material should be at least 2 inches (50 mm) or $1.4 \times \text{fillet radius}$ along each leg; have a thickness half of the solid side shell; taper for a length equal to at least three times the tape-in thickness; and include some sort of fillet material. Double bias knitted tapes with or without a mat backing are excellent choices for tape-in material. With primary reinforcement oriented at 45°, all fiberglass adds to the strength of the joint, while at the same time affording more flexibility. Figure 3-78 shows both double-bias tape-in versus conventional woven roving tape-in. When building up layers of reinforcements that have varying widths, it is best to place the narrowest plies on the bottom and work toward increasingly wide reinforcements. This reduces the amount of exposed edges.

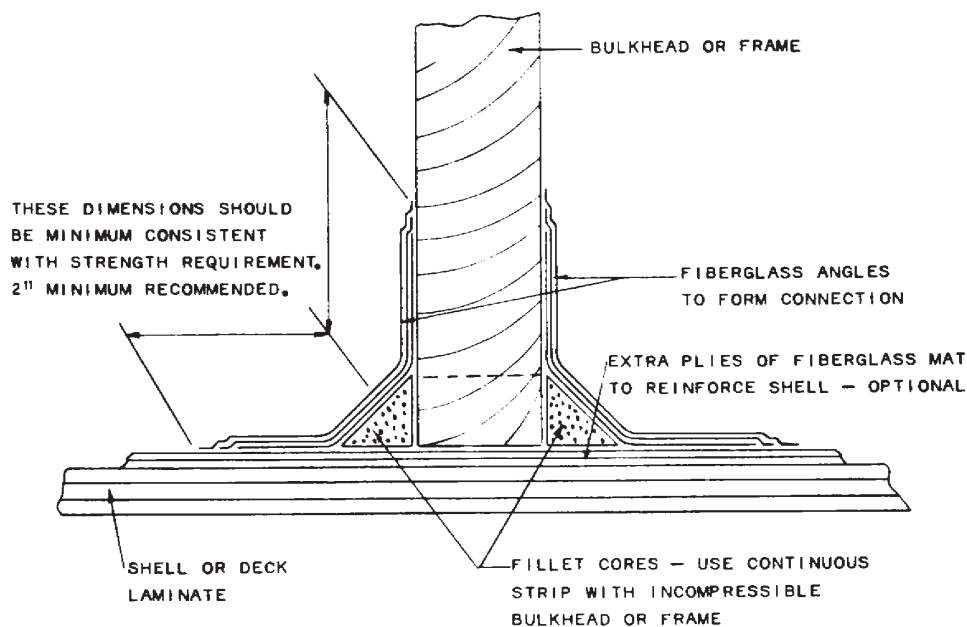


Figure 3-77 Connection of Bulkheads and Framing to Shell or Deck [Gibbs and Cox, *Marine Design Manual for FRP*]

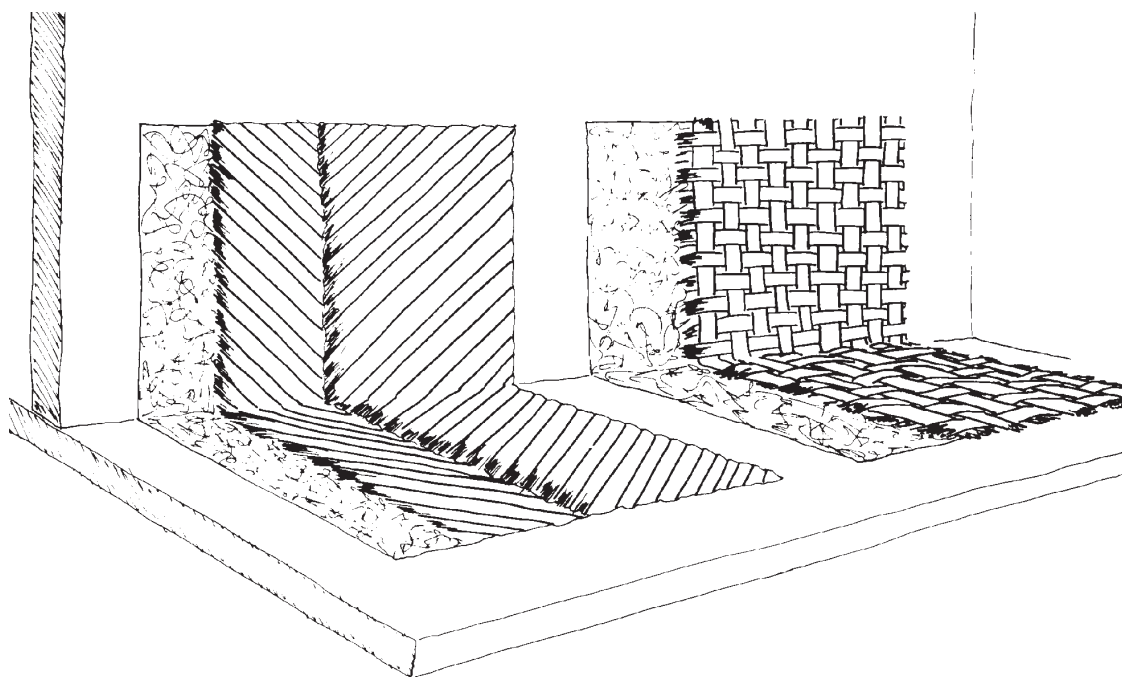


Figure 3-78 Double Bias and Woven Roving Bulkhead Tape-In [Knytex]

Stringers

Stringers in FRP construction can either be longitudinal or transverse and usually have a non-structural core that serves as a form. In general, continuity of longitudinal members should be maintained with appropriate cut-outs in transverse members. These intersections should be completely bonded on both the fore and aft side of the transverse member with a laminate schedule similar to that used for bonding to the hull.

Traditional FRP design philosophy produced stiffeners that were very narrow and deep to take advantage of the increased section modulus and stiffness produced by this geometry. The current trend with high-performance vehicles is toward shallower, wider stiffeners that reduce effective panel width and minimize stress concentrations. Figure 3-79 shows how panel span can be reduced with a low aspect ratio stiffener. Some builders are investigating techniques to integrally mold in stiffeners along with the hull's primary inner skin, thus eliminating secondary bonding problems altogether.

Regulatory agencies, such as ABS, typically specify stiffener scantlings in terms of required section moduli and moments of inertia. [3-6, 3-7, 3-22] Examples of a single skin FRP stiffener and a high-strength material stiffener with a cored panel are presented along with sample property calculations to illustrate the design process. These examples are taken from USCG NVIC No. 8-87. [3-22]

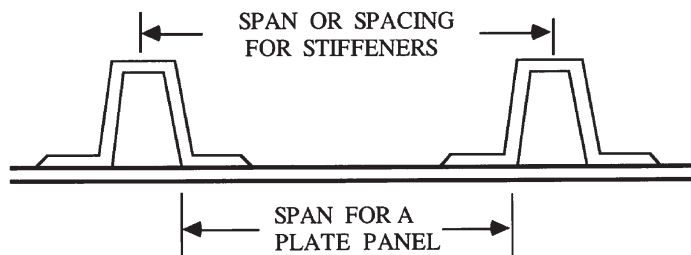


Figure 3-79 Reference Stiffener Span Dimensions [Al Horsmon, USCG NVIC No. 8-87]

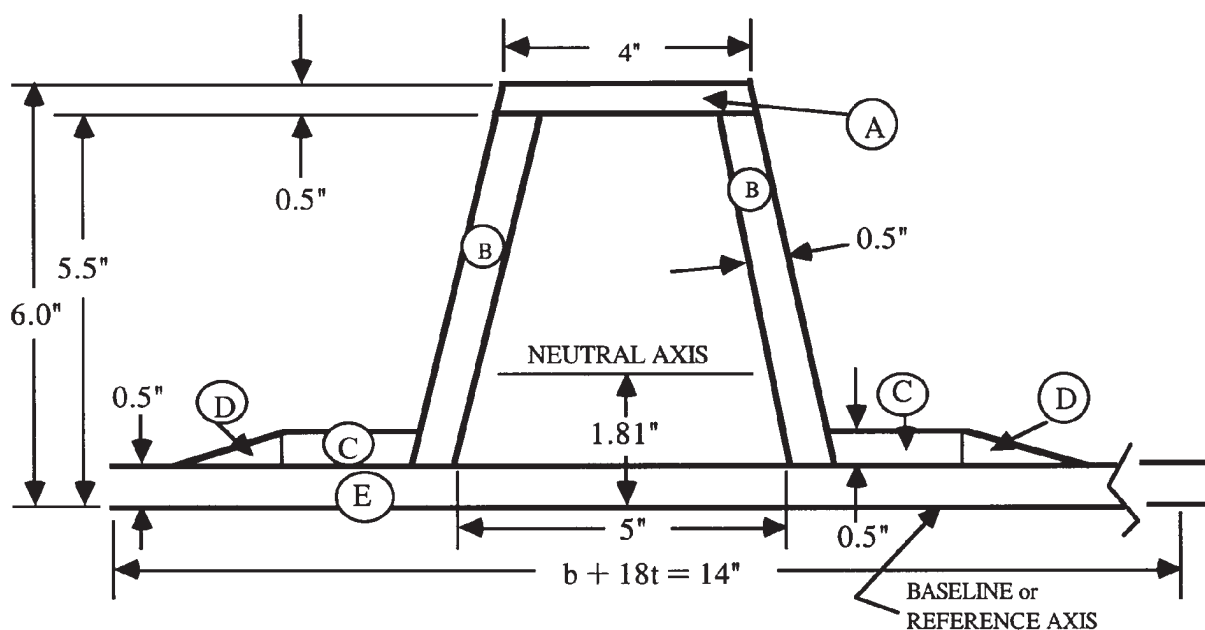


Figure 3-80 Stringer Geometry for Sandwich Construction [Al Horsmon, USCG NVIC No. 8-87]

Table 3-7 Example Calculation for Single Skin Stiffener

Item	b	h	A = b x h	d	Ad	Ad ²	i _o
A	4.00	0.50	2.00	5.75	11.50	66.13	0.04
B	0.50	5.10	2.55	3.00	7.65	23.95	5.31
B	0.50	5.10	2.55	3.00	7.65	23.95	5.31
C	2.00	0.50	1.00	0.75	0.75	0.56	0.02
C	2.00	0.50	1.00	0.75	0.75	0.56	0.02
D	3.00	0.50	0.75	0.67	0.50	0.33	0.01
E	14.00	0.50	7.00	0.25	1.75	0.44	0.15
Totals:			16.85		30.55	115.92	10.86

$$d_{NA} = \frac{\sum Ad}{\sum A} = \frac{30.55}{16.85} = 1.81 \text{ inches} \quad (3-87)$$

$$I_{NA} = \sum i_o + \sum Ad^2 - [Ad^2] = 10.86 + 115.92 - [16.85 \times (1.81)^2] = 71.58 \quad (3-88)$$

$$SM_{top} = \frac{I}{d_{NA top}} = \frac{71.58}{4.19} = 17.08 \text{ in}^3 \quad (3-89)$$

$$SM_{bottom} = \frac{I}{d_{NA bottom}} = \frac{71.58}{1.81} = 39.55 \text{ in}^3 \quad (3-90)$$

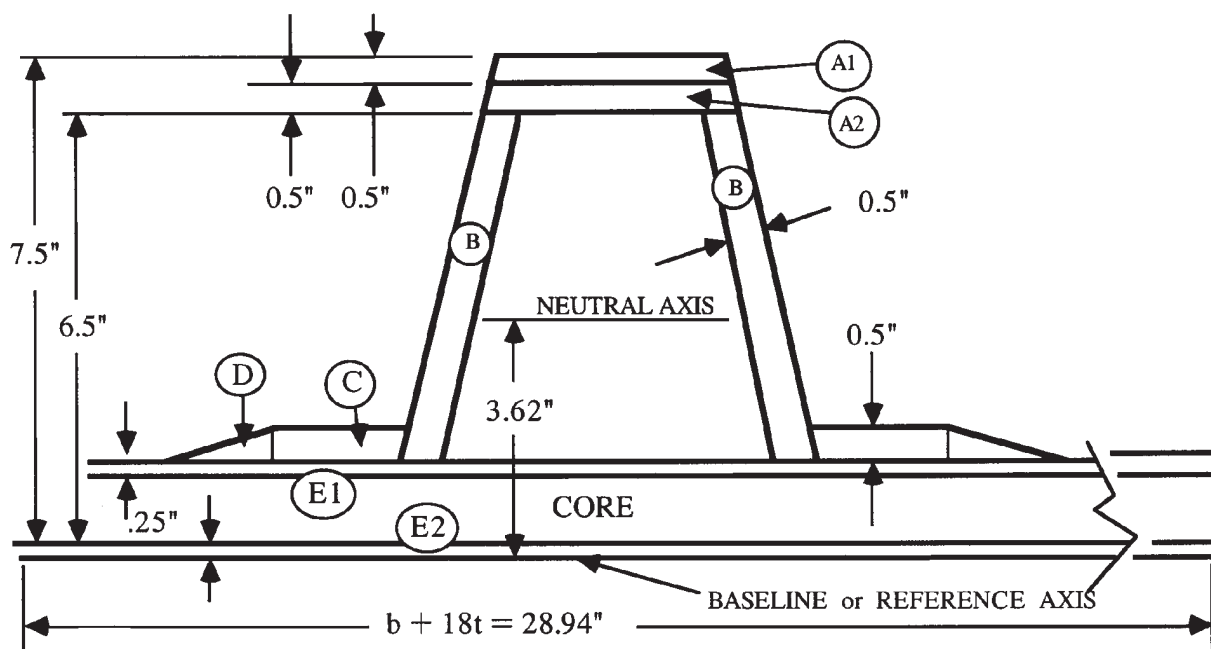


Figure 3-81 Stringer Geometry including High-Strength Reinforcement (3" wide layer of Kevlar[®] in the top) [Al Horsmon, USCG NVIC No. 8-87]

Table 3-8 High Strength Stiffener with Sandwich Side Shell

Item	b	h	A = b x h	d	Ad	Ad ²	i _o
A1	3.70	0.50	3.29*	7.25	23.85	172.93	0.069
A2	3.80	0.50	1.90	6.75	12.83	86.57	0.040
B	0.50	5.00	2.50	4.00	10.00	40.00	5.208
B	0.50	5.00	2.50	4.00	10.00	40.00	5.208
C	2.00	0.50	1.00	1.75	1.75	3.06	0.021
C	2.00	0.50	1.00	1.75	0.75	0.56	0.021
D	3.00	0.50	0.75	0.67	0.50	0.33	0.01
E1	28.94	0.25	7.23	1.37	9.95	13.68	0.038
E2	28.94	0.25	7.23	0.12	0.90	0.11	0.038
Totals:			27.40		70.53	357.24	10.65

$$d_{NA} = \frac{\sum Ad}{\sum A} = \frac{70.53}{27.40} = 2.57 \text{ inches} \quad (3-91)$$

$$I_{NA} = \sum i_o + \sum Ad^2 - [Ad^2] = 10.65 + 357.24 - [27.40 \times (2.57)^2] = 186.92 \quad (3-92)$$

$$SM_{top} = \frac{I}{d_{NA top}} = \frac{186.92}{4.93} = 37.9 \text{ in}^3 \quad (3-93)$$

$$SM_{bottom} = \frac{I}{d_{NA bottom}} = \frac{186.92}{2.57} = 72.73 \text{ in}^3 \quad (3-94)$$

SYMBOLS:

b = width or horizontal dimension

h = height or vertical dimension

d = height to center of A from reference axis

NA = neutral axis

i_o = item moment of inertia = $bh^3/12$

d_{NA} = distance from reference axis to real NA

I_{NA} = moment of inertia of stiffener and plate about the real neutral axis

The assumed neutral axis is at the outer shell so all distances are positive.

Note how the stiffened plate is divided into discrete areas and lettered.

Items B and C have the same effect on section properties and are counted twice.

Some simplifications were made for the vertical legs of the stiffener, item B . The item i_o was calculated using the equation for the I of an inclined rectangle. Considering the legs as vertical members would be a further simplification.

Item D is combined from both sides of the required bonding angle taper.

$$\text{Ratio of elastic moduli } E = \frac{E_{Kevlar^{\circledR}}}{E_{E-glass}} = \frac{9.8 \text{ msi}}{5.5 \text{ msi}}$$

* Effective area of Kevlar[®] compared to the E-glass = $3.7 \times 0.5 \times 1.78 = 3.29$

The overall required section modulus for this example must also reflect the mixed materials calculated as a modifier to the required section modulus:

$$SM_{Kevlar^{\circledR}} = SM_{E-glass} \times \frac{E_{Kevlar^{\circledR}}}{E_{E-glass}} \times \frac{\text{Ultimate Strength}_{E-glass}}{\text{Ultimate Strength}_{Kevlar^{\circledR}}}$$

$$\frac{E_{Kevlar^{\circledR}}}{E_{E-glass}} \times \frac{\text{Ultimate Strength}_{E-glass}}{\text{Ultimate Strength}_{Kevlar^{\circledR}}} = \frac{9.8 \text{ msi}}{5.5 \text{ msi}} \times \frac{110 \text{ ksi}}{196 \text{ ksi}} = 1.0$$

Reinforcing fibers of different strengths and different moduli can be limited in the amount of strength that the fibers can develop by the maximum elongation tolerated by the resin and the strain to failure of the surrounding laminate. Therefore, the strength of the overall laminate should be analyzed, and for marginal safety factor designs or arrangements meeting the minimum of a rule, tests of a sample laminate should be conducted to prove the integrity of the design. In this example, the required section modulus was unchanged but the credit for the actual section modulus to meet the rule was significant.

Stress Concentrations

Stress concentrations from out-of-plane point loads occur for a variety of reasons. The largest loads on a boat often occur when the boat is in dry storage, transported over land, removed from the water or placed into the water. The weight of a boat is distributed over the hull while the boat is in the water, but is concentrated at support points of relatively small area when the boat is out of the water. As an example, an 80 foot long 18 foot wide power boat weighing 130,000 pounds would probably experience a hydrostatic pressure of only a few psi. If the boat was supported on land by 12 blocks with a surface area of 200 square inches each, the support areas would see an average load of 54 psi. Equipment mounting, such as rudders, struts, engines, mast and rigging, booms, cranes, etc. can also introduce out-of-plane point loads into the structure through mechanical fasteners.

Hauling and Blocking Stresses

When a vessel is hauled and blocked for storage, the weight of the vessel is not uniformly supported as in the water. The point loading from slings and cradle fixtures is obviously a problem. The overall hull, however, will be subject to bending stresses when a vessel is lifted with slings at two points. Except in extreme situations, in-service design criteria for small craft up to about 100 feet should be more severe than this case. When undergoing long term storage or over-land transit, consideration must be given to what fixtures will be employed over a given period of time. Creep behavior described in Chapter Six will dictate long-term structural response, especially under elevated temperature conditions. Large unsupported weights, such as machinery, keels or tanks, can produce unacceptable overall bending moments in addition to the local stress concentrations. During transportation, acceleration forces transmitted through the trailer's support system can be quite high. The onset of fatigue damage may be quite precipitous, especially with cored construction.

Engine Beds

If properly fabricated, engine beds in FRP vessels can potentially reduce the transmission of machinery vibration to the hull. Any foundation supporting propulsion machinery should be given the same attention afforded the main engine girders.

As a general rule, engine girders should be of sufficient strength, stiffness and stability to ensure proper operation of rotating machinery. Proper bonding to the hull over a large area is essential. Girders should be continuous through transverse frames and terminate with a gradual taper. Laminated timbers have been used as a core material because of excellent damping properties and the ability to hold lag bolt fasteners. Consideration should be given to bedding lag bolts in resin to prevent water egress. Some builders include some metallic stock between the core and the laminate to accept machine screws. If this is done, proper care should be exercised to guarantee that the metal remains bonded to the core. New, high density PVC foam cores offer an attractive alternative that eliminates the concern over future wood decay.

Hardware

Through-bolts are always more desirable than self-tapping fasteners. Hardware installations in single skin laminates is fairly straightforward. Backing plates of aluminum or stainless steel are always preferable over simple washers. If using only oversized washers, the local thickness should be increased by at least 25%. [3-23] The strength of hardware installations should be consistent with the combined load on a particular piece of hardware. In addition to shear and normal loads, applied moments with tall hardware must be considered. Winches that are mounted on pedestals are examples of hardware that produce large overturning moments.

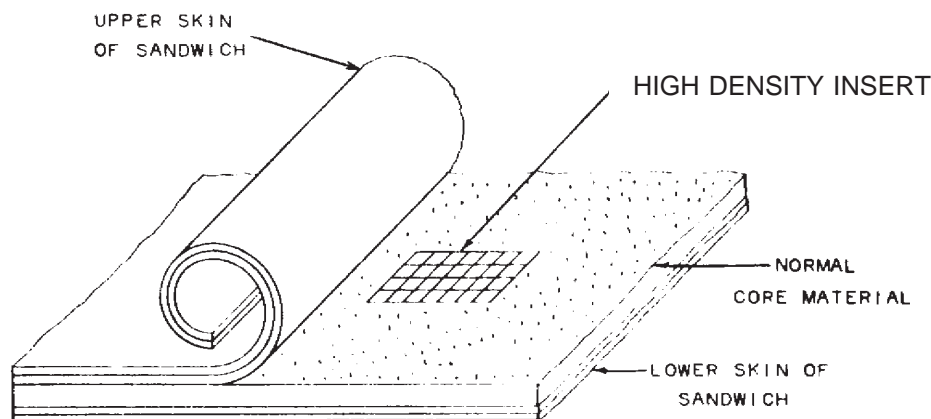


Figure 3-82 High Density Insert for Threaded or Bolted fasteners in Sandwich Construction [Gibbs and Cox, *Marine Design Manual for FRP*]

Hardware installation in cored construction requires a little more planning and effort. Low density cores have very poor holding power with screws and tend to compress under the load of bolts. Some builders simply taper the laminate to a solid thickness in way of planned hardware installations. This technique has the drawback of generally reducing the section modulus of the deck unless a lot of solid glass is used. A more efficient approach involves the insertion of a higher density core in way of planned hardware. In the past, the material of choice was plywood, but high density PVC foam will provide superior adhesion. Figure 3-82 illustrates this technique.

Hardware must often be located and mounted after the primary laminate is complete. To eliminate the possibility of core crushing, a compression tube as illustrated in Figure 3-83 should be inserted.

Nonessential hardware and trim, especially on small boats, is often mounted with screw fasteners. Table 3-9 is reproduced to provide some guidance in determining the potential holding force of these fasteners [3-24]. This table is suitable for use with mat and woven roving type laminate with tensile strength between 6 and 25 ksi; compressive strength between 10 and 22 ksi; and shear strength between 10 and 13 ksi.

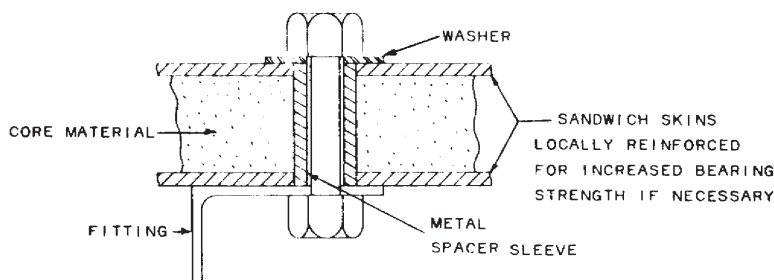


Figure 3-83 Through Bolting in Sandwich Construction [Gibbs and Cox, *Marine Design Manual for FRP*]

**Table 3-9 Holding Forces of Fasteners in Mat/Polyester Laminates
[Gibbs and Cox, Marine Design Manual for FRP]**

Thread Size	Axial Holding Force				Lateral Holding Force			
	Minimum		Maximum		Minimum		Maximum	
	Depth (ins)	Force (lbs)	Depth (ins)	Force (lbs)	Depth (ins)	Force (lbs)	Depth (ins)	Force (lbs)
Machine Screws								
4 - 40	.1250	40	.3125	450	.0625	150	.1250	290
6 - 32	.1250	60	.3750	600	.0625	180	.1250	380
8 - 32	.1250	100	.4375	1150	.0625	220	.1875	750
10 - 32	.1250	150	.5000	1500	.1250	560	.2500	1350
¼ - 20	.1875	300	.6250	2300	.1875	1300	.3125	1900
⅕ - 18	.1875	400	.7500	3600	.1875	1600	.4375	2900
⅜ - 16	.2500	530	.8750	5000	.2500	2600	.6250	4000
⅞ - 14	.2500	580	1.0000	6500	.3125	3800	.7500	5000
½ - 13	.2500	620	1.1250	8300	.3750	5500	.8750	6000
⅙ - 12	.2500	650	1.2500	10000	.4375	6500	.9375	8000
⅝ - 11	.2500	680	1.3750	12000	.4375	6800	1.0000	11000
¾ - 10	.2500	700	1.5000	13500	.4375	7000	1.0625	17000
Self-Tapping Thread Cutting Screws								
4 - 40	.1250	80	.4375	900	.1250	250	.1875	410
6 - 32	.1250	100	.4375	1100	.1250	300	.2500	700
8 - 32	.2500	350	.7500	2300	.1875	580	.3750	1300
10 - 32	.2500	400	.7500	2500	.1875	720	.4375	1750
¼ - 20	.3750	600	1.0625	4100	.2500	1600	.6250	3200
Self-Tapping Thread Forming Screws								
4 - 24	.1250	50	.3750	500	.1250	220	.1875	500
6 - 20	.1875	110	.6250	850	.1250	250	.2500	600
8 - 18	.2500	180	.8125	1200	.1875	380	.3125	850
10 - 16	.2500	220	.9375	2100	.2500	600	.5000	1500
14 - 14	.3125	360	1.0625	3200	.2500	900	.6875	2800
⅙ - 18	.3750	570	1.1250	4500	.3125	1800	.8125	4400
⅜ - 12	.3750	700	1.1250	5500	.3750	3600	1.0000	6800

Sandwich Panel Testing

Background

Finite element models can be used to calculate panel deflections for various laminates under worst case loads [3-25,3-26], but the accuracy of these predictions is highly dependent on test data for the laminates. Traditional test methods [3-27] involve testing narrow strips, using ASTM standards outlined in Chapter Four. Use of these tests assumes that hull panels can be accurately modeled as a beam, thus ignoring the membrane effect, which is particularly important in sandwich panels [3-28]. The traditional tests also cause much higher stresses in the core, thus leading to premature failure [3-29].

A student project at the Florida Institute of Technology investigated three point bending failure stress levels for sandwich panels of various laminates and span to width ratios. The results were fairly consistent for biaxial (0° , 90°) laminates, but considerable variation in deflection and failure stress for double bias ($\pm 45^\circ$) laminates was observed as the aspect ratio was changed. Thus while the traditional tests yield consistent results for biaxial laminates, the test properties may be significantly lower than actual properties, and test results for double bias and triaxial laminates are generally inaccurate.

Riley and Isley [3-30] addressed these problems by using a new test procedure. They pressure loaded sandwich panels, which were clamped to a rigid frame. Different panel aspect ratios were investigated for both biaxial and double bias sandwich laminates. The results showed that the double bias laminates were favored for aspect ratios less than two, while biaxial laminates performed better with aspect ratios greater than three. Finite element models of these tests indicated similar results, however, the magnitude of the deflections and the pressure at failure was quite different. This was probably due to the method of fastening the edge of the panel. The method of clamping of the edges probably caused local stress concentrations and could not be modeled by either pinned- or fixed-end conditions.

Pressure Table Design

The basic concept of pressure loading test panels is sound, however, the edges or boundary conditions need to be examined closely. In an actual hull, a continuous outer skin is supported by longitudinal and transverse framing, which defines the hull panels. The appropriate panel boundary condition is one which reflects the continuous nature of the outer skin, while providing for the added stiffness and strength of the frames. One possible solution to this problem is to include the frame with the panel, and restrain the panel from the frame, rather than the panel edges. Also, extending the panel beyond the frame can approximate the continuous nature of the outer skin.

A test apparatus, consisting of a table, a water bladder for pressurizing the panel, a frame to constrain the sides of the water bladder, and framing to restrain the test panel, was developed and is shown in Figure 3-84. The test panel is loaded on the “outside,” while it is restrained by means of the integral frame system. The pressurization system can be operated either manually or under computer control, for pressure loading to failure or for pressure cycling to study fatigue.

Test Results

Sandwich laminates using four different reinforcements and three aspect ratios were constructed for testing. All panels used non-woven E-glass, vinyl ester resin and cross-linked

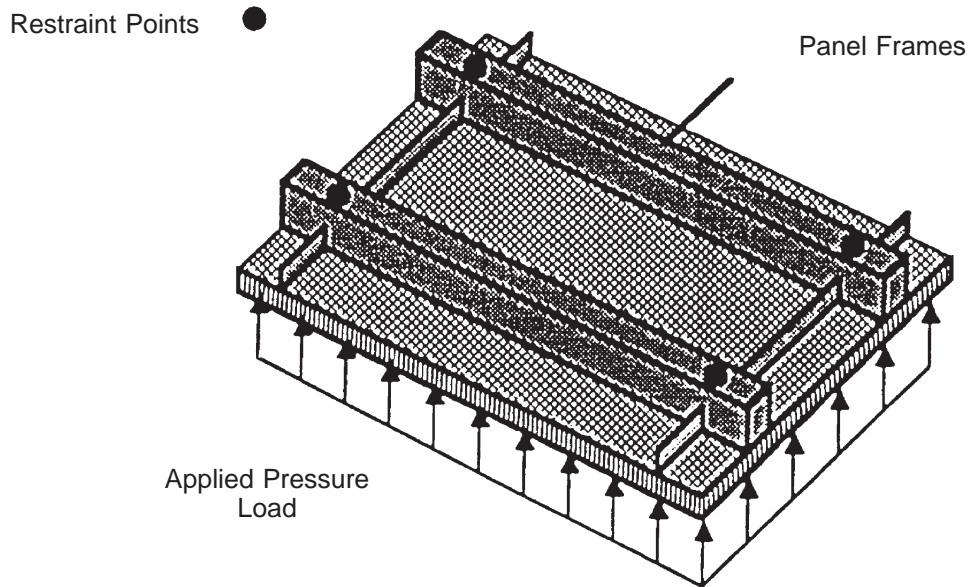


Figure 3-84 Schematic Diagram of Panel Testing Pressure Table [Reichard]

PVC foam cores over fir frames and stringers. The panels were loaded slowly (approximately 1 psi per minute) until failure.

MSC/NASTRAN, a finite element structural analysis program, was used to model the panel tests. The models were run using two different boundary conditions, pinned edges and fixed edges. The predicted deflections for fixed- and pinned-edge conditions along with measured results are shown in Figure 3-85.

The pinned-edge predictions most closely model the test results. Other conclusions that can be made as a result of early pressure table testing include:

- Quasi-isotropic laminates are favored for square panels.
- Triaxial laminates are favored for panels of aspect ratios greater than two.

Deflection increase with aspect ratio until asymptotic values are obtained. Asymptotic values of deflection are reached at aspect ratios between 2.0 and 3.5.

The pressure table test method provides strength and stiffness data for the panel structure but does not provide information about specific material properties. Therefore, the test is best suited for comparing candidate structures.

Testing of Structural Grillage Systems

Figure 3-86 shows a hat-stiffened panel subjected to in-plane and out-of-plane loads tested at the U.S. Naval Academy. The structure modeled would be typical of a longitudinally stiffened hull panel. Note the half-sine wave pattern of the collapsed skin even as the panel was subjected to out-of-plane loads from the water bladder with nominal loading. After the panel separated from the stiffeners, the hat sections experienced shear failure.

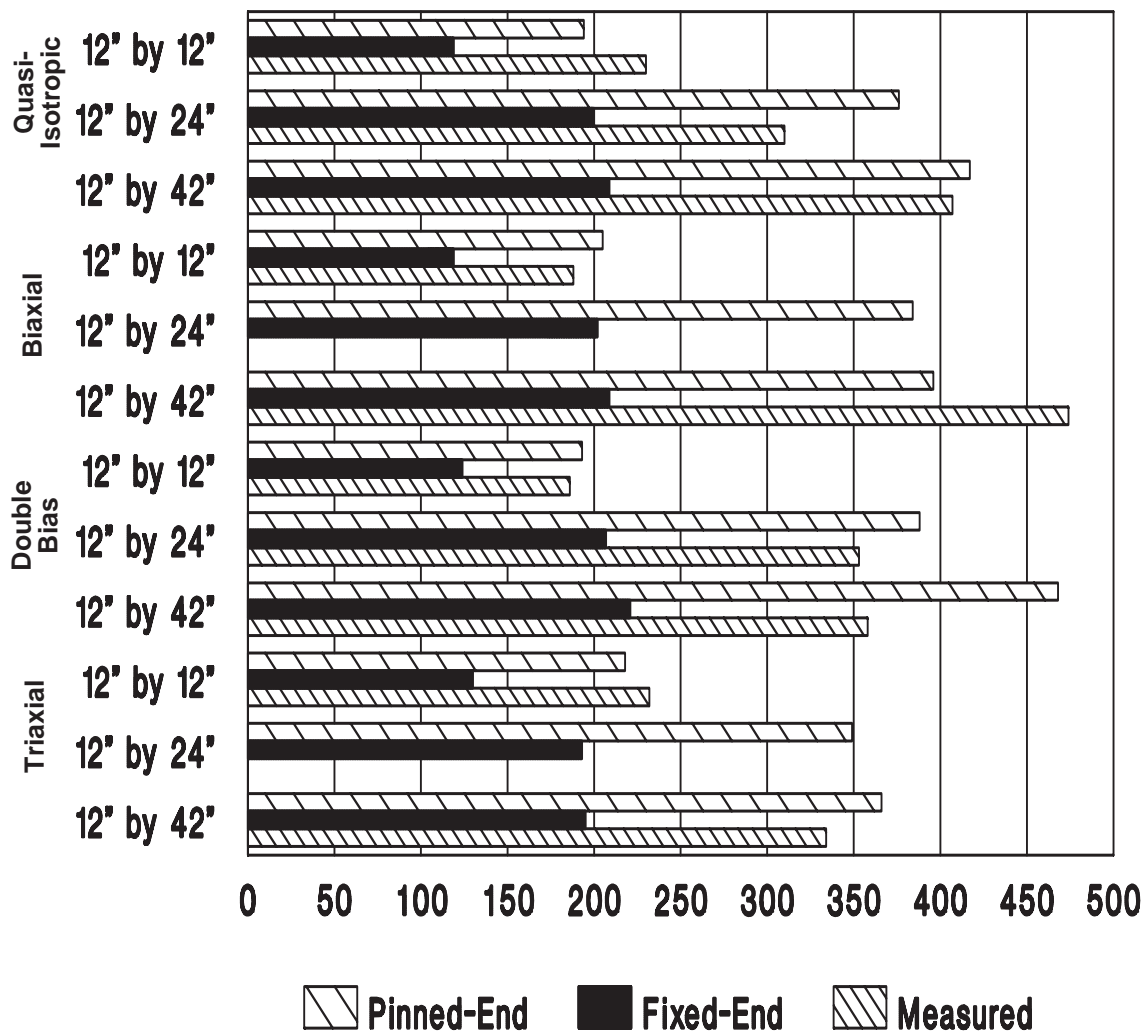


Figure 3-85 Computed and Measured Deflections (mils) of PVC Foam Core Panels Subjected to a 10 psi Load [from Reichard, Ronnal P., "Pressure Panel Testing of GRP Sandwich Panels," MACM' 92 Conference, Melbourne, FL, March 24-26, 1992.

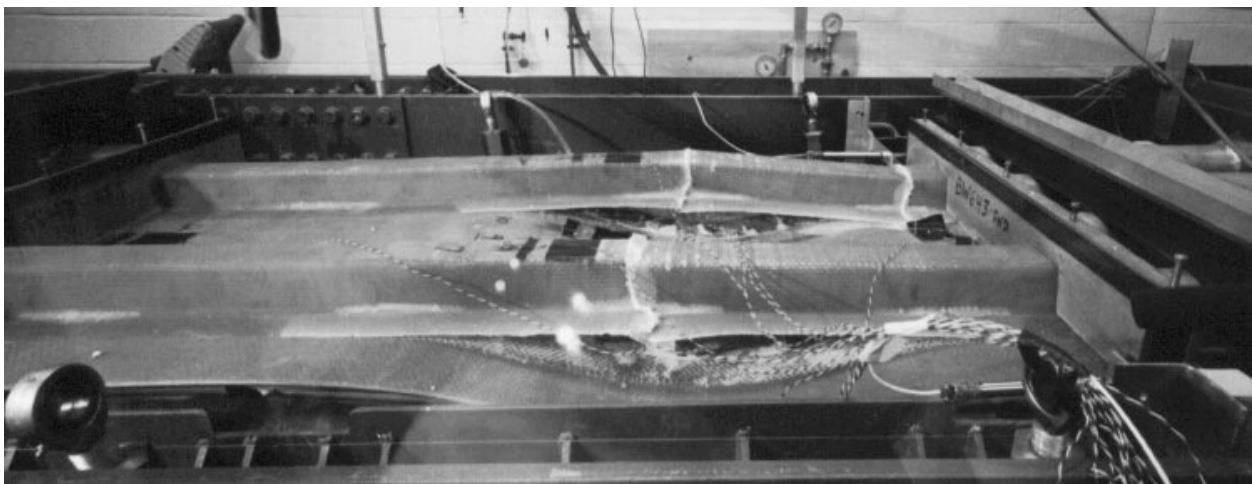


Figure 3-86 Hat-Stiffened Panel Tested to Failure at the U.S. Naval Academy

Hydromat Test System (HTS)

Bill Bertelsen of Gougeon Brothers and Dave Sikarskie of Michigan Technological University have developed a two dimensional panel testing device and governing design equations. The test device, shown in Figure 3-87, subjects panels to out-of-plane loads with simply-supported end conditions. The boundary conditions have been extended to cover sandwich panels with soft cores, thereby enabling characterization of sandwich panels both elastically and at failure. A methodology has been developed for obtaining numerical and experimental values for bending and core shear rigidities, which both contribute to measured deflections.

In the simplest form, the deflection, δ , is given as:

$$\delta = \frac{c_1}{B} + \frac{c_2}{S} \quad (3-95)$$

where:

$$\begin{aligned} c_1 \& c_2 &= \text{constants} \\ B &= \text{bending stiffness} \\ S &= \text{core shear stiffness} \end{aligned}$$

Tests were run on panels with varying stiffness to verify the methodology. Table 3-10 summarizes some results, showing the close agreement between experimental and theoretical overall bending and core shear stiffness.

Table 3-10 Summary of Experimental and Theoretical Bending and Shear Stiffness [Bertlesen, Eyre and Sikarskie, *Verification of HTS for Sandwich Panels*]

Panel	Bladder Pressure (kPa)	Total HTS Deflection	$(\epsilon_x + \epsilon_y)$ Exp. μ strain	B, exp (10^4 nM)	B, theory (10^4 nM)	S, exp (10^4 nM)	S, theory (10^4 nM)
1	31.0	2.78	463	2.08	2.52	3.48	3.72
2	48.3	2.85	719	2.12	2.55	6.43	5.24
3	75.8	2.49	1062	2.33	2.43	17.68	17.04

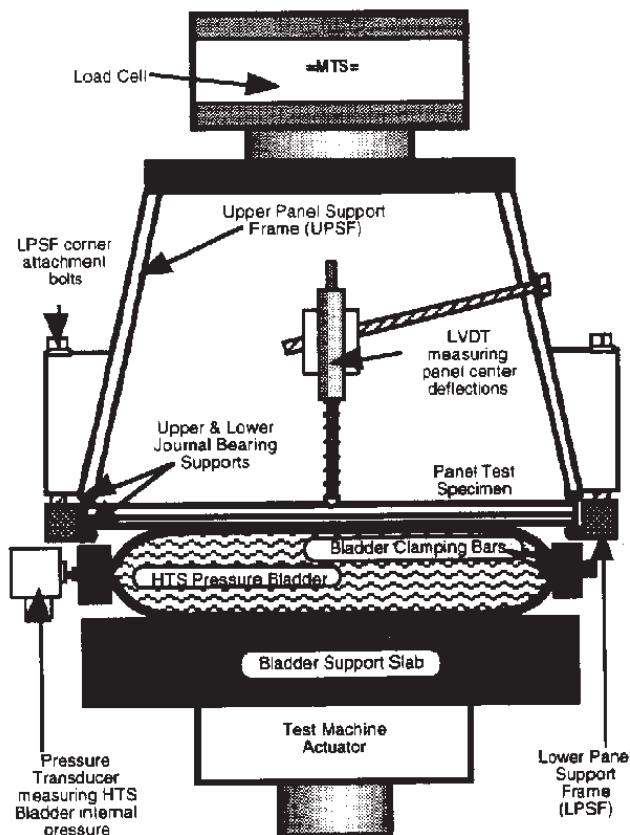


Figure 3-87 Schematic Diagram of the Hydromat Test System [Bertlesen & Sikarskie]